

Localized Lower Hybrid Acceleration of Ionospheric Plasma

P. M. Kintner, J. Vago, and S. Chesney
Cornell University, Ithaca, New York 14853

R. L. Arnoldy and K. A. Lynch
University of New Hampshire, Durham, New Hampshire 03824

C. J. Pollock and T. E. Moore
Marshall Space Flight Center, Huntsville, Alabama 35812
 (Received 17 October 1991; revised manuscript received 10 February 1992)

We report observations of the transverse acceleration of ions in localized regions of intense lower hybrid waves at altitudes near 1000 km in the auroral ionosphere. The acceleration regions are thin filaments with dimensions across geomagnetic field lines of about 50–100 m corresponding to 5–10 thermal ion gyroradii or one hot ion gyroradius. Within the acceleration region lower hybrid waves reach peak-to-peak amplitudes of 100–300 mV/m and ions are accelerated transversely with characteristic energies of the order of 10 eV. These observations are consistent with theories of lower hybrid wave collapse.

PACS numbers: 94.20.-y, 52.40.Db

Ion acceleration and heating are important aspects of both laboratory plasma experiments and space plasma experiments. From the viewpoint of space plasmas, ion heating is necessary to account for the plasma mass in the terrestrial magnetosphere. For example, O^+ ions of a few keV to several tens of keV are known to populate the Earth's magnetosphere [1]. Since O^+ must originate from the ionosphere where O^+ is gravitationally bound, there must exist a mechanism to eject the O^+ ions. On the other hand, O^+ ions are also known to be accelerated transversely on auroral magnetic field lines at altitudes above 500 km [2]. The characteristic energy of the accelerated O^+ ions is 10–100 eV, which is sufficient to eject the ions into the magnetosphere [3].

A successful theory to produce transversely accelerated ions (TAI) must operate below 2000-km altitude where O^+ densities are adequate. Recently, theories to explain ion conics have employed O^+ gyroresonant waves and plasma wave observations above 6000-km altitude which are extrapolated to the source region below 2000-km altitude [4]. On the other hand, lower hybrid waves generated by auroral electrons can also produce TAI [5]. However, observation of the required lower hybrid waves has been problematic [6,7].

In this Letter we demonstrate that TAI in the source region are produced by intense lower hybrid waves in thin filaments, about 50 m thick, which are oriented along geomagnetic field lines. The data from which we primarily draw our conclusions come from the TOPAZ 3 (topside probe of the auroral zone) sounding rocket, although similar phenomena have been observed by two other sounding-rocket experiments [3,8]. TOPAZ 3 was launched northward from Poker Flat, Alaska, at 0912 GMT on 12 February 1991. It reached an altitude of 1067 km and overflow several auroral arcs during a moderate substorm. The instrumentation included a two-axis plasma-wave receiver and interferometer operating from 0 to 20 kHz. The plasma-wave receiver em-

ployed four 1-m radially directed antennas each of which was located 3.25 m from the payload. The particle instruments consisted of a pitch-angle-imaging electrostatic ion analyzer (HEEPS 1) operating from 7 to 880 eV with 125-ms time resolution, a fixed-mass (H^+ and O^+) pitch-angle-imaging analyzer (BEEPS) operating up to 600 eV with 250-ms time resolution, a pitch-angle-imaging electrostatic electron analyzer (HEEPS 2) operating from 10 eV to 17 keV with 250-ms time resolution, a scanning ion mass spectrometer (STICS) operating from 0.1 to 100 eV with 10-s time resolution, and a fixed-bias Langmuir probe.

The ionospheric plasma conditions for the data presented herein were a density of roughly $4 \times 10^3 \text{ cm}^{-3}$ in a magnetic field of 0.36 G, which yields $f_{pe} = 5.7 \times 10^5 \text{ Hz}$ and $f_{ce} = 1.0 \times 10^6 \text{ Hz}$. The measured O^+ density was $4 \times 10^3 \text{ cm}^{-3}$ and the measured H^+ density was $3 \times 10^2 \text{ cm}^{-3}$. These ion densities imply a lower hybrid frequency of 4500 Hz compared to the measured value of 4300 Hz evident in Fig. 1. Although the ion temperatures have not yet been extracted from the TOPAZ 3 data, during a previous experiment (TOPAZ 2) and in similar ionospheric conditions the ion temperatures varied between 3500 and 4000 K. The electron temperature was not measured but typical temperatures for this environment are $(1-5) \times 10^3 \text{ K}$.

Figure 1 shows an example of 2 s of HEEPS 1 ion data, plasma-wave data, and Langmuir probe data. The upper panel (sweep and counts/ms) shows the energy step for the HEEPS 1 analyzer and the count rate at each step. The middle panel (pitch angle) shows the count rate as a gray scale for different pitch angles with respect to the geomagnetic field as a function of time. The three blank stripes correspond to detector struts slowing rotating with time. At 472.0 and 472.4 s are two brief periods of large count rates corresponding to TAI. These two events occur in a time span of the order of or less than the detector sweep rate of 125 ms. A separate fixed-energy

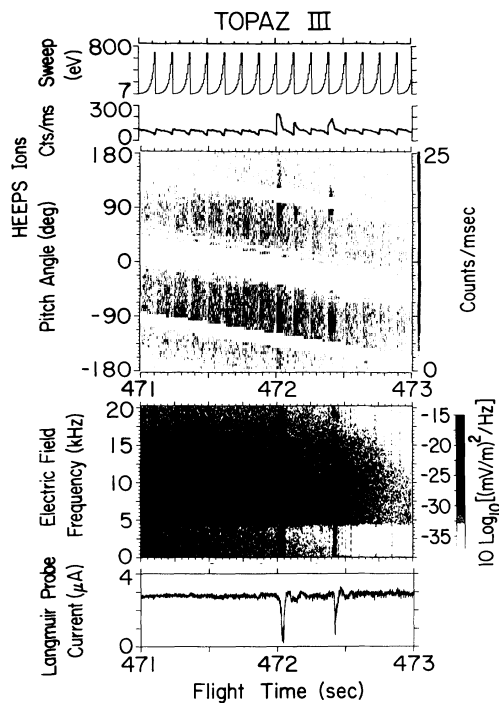


FIG. 1. 2 s of sounding-rocket data at 1012-km altitude. The upper panel (sweep and labeled counts/ms) shows the count rate of a pinch-angle-imaging ion analyzer and the ion energy. The panel labeled "pitch angle" shows as a gray scale, the ion count rate as a function of pitch angle with respect to the geomagnetic field. The panel labeled "electric field" shows the electric-field power spectrum as a gray scale. The bottom panel shows the current drawn by a fixed-bias (+5 V) Langmuir probe.

(13 eV) detector yielded a typical value of 50 ms for the duration of these events. In addition, the HEEPS 1 ion data in the middle panel demonstrate that the TAI were accelerated near 90° pitch angle. Several hundred of these TAI events occurred during the flight; the more energetic events occurred over apogee at an average rate of once per second. The BEEPS instrument indicated that both O^+ and H^+ were accelerated with properties that varied from event to event [9]. The O^+ distributions were tail accelerated transversely while the H^+ distributions were primarily accelerated in the transverse direction with less acceleration in the parallel direction. Occasionally the H^+ distributions displayed evidence of tail heating in the transverse direction.

We now turn to the electric-field data which were measured simultaneously with the ion events. In Fig. 1, the panel labeled "electric field" shows the power up to 20 kHz received by a 1-m dipole antenna which was slowly spinning with respect to the geomagnetic field. At 472.8 s it was roughly aligned with the geomagnetic field which explains the minimum in received power at that time. The nearly continuous band with a low-frequency cutoff at 4.3 kHz was auroral hiss which is typically produced

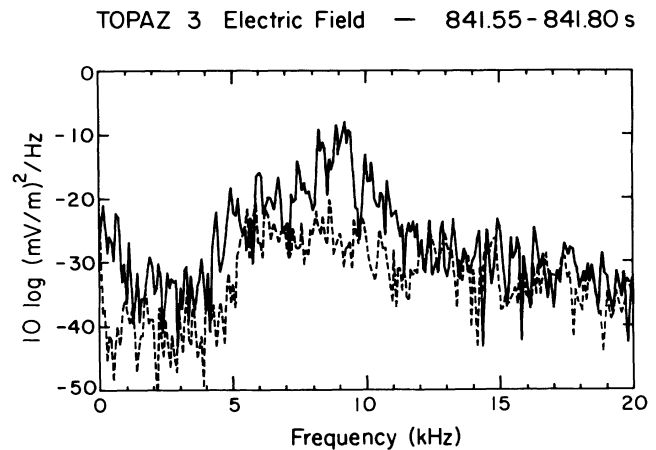


FIG. 2. The power spectrum of a lower hybrid wave impulse (solid line) and a power spectrum 50 ms later (dashed line).

by field-aligned auroral electron beams with energies of 100 eV to a few keV [10]. The cutoff frequency of 4.3 kHz corresponds to the lower hybrid frequency. Coincident with the two TAI events at 472.0 and 472.4 s are two wave events which appear to be broadband, impulsive increases in wave power. We discuss the properties of these plasma-wave impulses next, which in previous work were called spikelets [8].

Both the auroral hiss and the plasma-wave impulses had substantially larger amplitudes than predicted from previous measurements. The saturation level of the electric-field instrument was set at 80 mV/m peak to peak and most plasma-wave impulse signals were clipped by the receiver. The exceptions were when the antenna was within 30° of being aligned to the geomagnetic field and when the wave impulse amplitudes were small. The power spectrum of one such exception is shown in Fig. 2. This wave impulse event occurred at 841.5 s at an altitude of 855 km and was simultaneously accompanied by a TAI event. The ambient lower hybrid frequency for this time was 5.5 kHz. The power spectrum exhibits a clear peak at 9 kHz, somewhat above the lower hybrid frequency which is typical of the wave events. Examination of time series data revealed a wave train about 25–30 ms long with peak-to-peak amplitudes briefly reaching the clipping level of ± 40 mV/m. Since the angle between the antenna and the geomagnetic field was 26° and these electric fields were typically measured to be perpendicular or nearly perpendicular to the geomagnetic field, the wave impulse amplitude briefly attained 180 mV/m peak to peak. Other measurements characteristic of the events in Fig. 1 suggest that peak-to-peak electric-field amplitudes reached 300–400 mV/m. Electric-field probes spaced around the payload implied that the power below about 4 kHz was directed radially away from the payload and therefore not geophysical. The same spaced probes indicated that the power above 5 kHz was coherent with wavelengths of 2 to 20 m and was geo-

physical in origin. Between 4 and 5 kHz a mixture of radial electric fields and geophysical electric fields was present.

The TAI events and plasma-wave impulses occurred simultaneously in a majority of the examples but a significant fraction were not simultaneous. Outside regions of auroral electron precipitation, where the VLF hiss was weaker, lower hybrid wave impulses with smaller amplitudes were frequently observed without TAI. Within regions of auroral electron precipitation and above 500-km altitude about (15–25)% of the TAI events were not accompanied by plasma-wave impulses.

The lower panel of Fig. 1, labeled “Langmuir probe,” illustrates another feature of the TAI and lower hybrid impulse events. The Langmuir probe is a 2.5-cm \times 1.8-cm cylinder located 1.4 m from the payload and biased at +5 V with respect to the payload. A characteristic feature of the TAI events when simultaneously accompanied by wave impulse events is a decrease in the Langmuir probe current. For the events of Fig. 1 the current dropped by nearly an order of magnitude. This was an extreme example. Most examples exhibited currents which decreased by a few tens of percent. Interpreting the Langmuir probe current is difficult as the spaced electric-field probes implied that there were sheaths around the payload during the simultaneous TAI and wave impulse events. The Debye length was no more than 10–20 cm depending on the density and electron temperature chosen, from which we infer that the payload sheath should not extend from the payload to the Langmuir probe. Furthermore, no current decreases were observed when TAI events were not accompanied by plasma-wave impulses, which suggests that the accelerated ions could not be responsible for the current decrease. Detailed examination of the temporal features of the Langmuir probe current and sheath electric fields suggests major differences between the two records during the simultaneous events. Hence we conclude that at least a major fraction of the current decrease was not associated with payload sheaths and that the current decreases are evidence of plasma density depletions of the order of (10–50)%.

In space plasma experiments there are typically two difficult issues in interpreting experimental data: the direction of energy flow (“chicken and egg” paradox) and spatial properties versus temporal properties. In our case the issue of energy flow reduces to the question of whether the TAI produce the lower hybrid wave impulses or vice versa. This question is resolved by comparing the TAI events with the lower hybrid impulses. On the up leg and over apogee, when the TAI were most energetic and their fluxes were the largest and when the lower hybrid impulses had the largest amplitudes, about (15–25)% of the TAI events were not accompanied by lower hybrid impulses. Since TAI occur without lower hybrid impulses, it seems unlikely that the TAI were producing

the impulses. If the lower hybrid impulses are producing the TAI, TAI should be measured frequently without being accompanied by plasma-wave impulses since accelerated ions will drift upward and out of the acceleration volume via the mirror force. In addition, spectral power within the impulses was observed at a frequency of 5 kHz and a wavelength of 2 m which was capable of resonating with and accelerating the ions. We conclude that our measurements best fit the hypothesis that the plasma-wave impulses produced the TAI.

For the question of space versus time we need to resolve whether the 50–100-ms events are temporal or spatial. Since the payload speed across geomagnetic field lines was about 1 km/s, a fixed object of 1-m dimension would be observed as a 1-ms event in the payload reference frame. In our case the ambiguity is removed by considering the lifetime of an accelerated ion on a length of geomagnetic field line. A typical upward velocity (parallel to \mathbf{B}) of the transversely accelerated ions was a few km/s. Once accelerated, the upward movement of the ion is collisionless and it should proceed more or less unimpeded for thousands of kilometers. Since most [(75–85)%] of the TAI events were accompanied by lower hybrid wave impulses, the acceleration length along \mathbf{B} is most likely a large fraction of the distance between the minimum observed altitude and apogee ($\cong 500$ km). If this were not true, most TAI events would not be accompanied by lower hybrid wave impulses. For an acceleration length of 100 km, transversely accelerated ions will take tens of seconds to exit the acceleration region. Hence, the events measured by the payload must be spatial, are thin filaments, and have diameters the order of 50–100 m.

Given that the lower hybrid wave impulses produced the TAI, there were only two possible sources of free energy for the wave impulses: either the observed VLF hiss or unobserved electrons below the 10-eV threshold energy of the electrostatic analyzer. Above 10 eV there was no particular association of the wave impulse events with electron distributions although normal auroral electron precipitation occurred off and on throughout the flight and during the wave impulse events. In a few cases there were almost no observed electrons above the threshold energy of 10 eV. It seems unlikely that unobservable electron distribution features below 10 eV were producing the wave impulses, although we cannot strictly rule out thermal electron drift as a source of free energy.

This leaves the auroral hiss as the probable source of energy for the wave impulses. Auroral hiss has both an electromagnetic component (whistler mode) and an electrostatic component (lower hybrid resonance) depending on the angle of propagation. Previous work [11–13] suggests that lower hybrid waves can condense via the ponderomotive force and produce transverse ion acceleration. Some of the data herein support this hypothesis such as increases in lower hybrid wave amplitude, short wave-

lengths ($k\rho_i \gg 1$), plasma density depletions, and transverse ion acceleration. An approximate threshold for wave condensation is $(W/nkT_e)m_i/m_e > 1$. We infer from our data that outside regions of TAI, $(W/nkT_e)m_i/m_e \cong 1$, while inside regions of TAI, $(W/nkT_e)m_i/m_e \cong 30$. This suggests that the VLF hiss was marginally stable to collapse and occasionally did collapse into lower hybrid impulses. On the other hand, linear wave mode conversion could also be responsible for the wave impulses. At this time our measurements cannot distinguish between these two possibilities.

Our measurements are consistent with satellite measurements of TAI assuming a spatial interpretation for the sounding-rocket measurements. The narrow regions of TAI and wave impulses were sprinkled densely throughout the flight of TOPAZ 3. By time averaging over the sounding-rocket events and assuming no TAI between the events, we calculate that for one ion acceleration event per second, a typical average flux of ions heated above 7 eV is 2×10^7 ions $(\text{cm}^2 \text{ssr})^{-1}$. A satellite with a velocity of 8 km/s would average over these events by measuring $\frac{1}{8}$ fewer ions per event but measuring 8 times more events per unit time to yield the same average flux as that measured on the sounding rocket. Our result agrees exceptionally well with Fig. 4 of Ref. [14] where TAI were observed from a satellite (ISIS-1) with peak fluxes, integrated between 6.2 and 842 eV, of 2×10^7 ions $(\text{cm}^2 \text{ssr})^{-1}$ at an altitude of 1450 km.

This work has benefited from discussions with T. Chang, J. Maggs, G. Morales, C. Seyler, and V. Shapiro. We would like to acknowledge support received at Cornell from NASA Grant No. NAG-5-601 and ONR Grant No. N00014-90-C-0003, at the University of New Hampshire by NASA Grant No. NAG6-12, and at Marshall Space Flight Center under NASA RTOP No.

435-11-00-19. The STICS mass analyzer and stepping power supplies were developed by the University of Texas at Dallas. The TOPAZ sounding-rocket experiment was made possible by the NASA/Wallops Flight Facility.

-
- [1] G. Gloeckler, B. Wilken, W. Stüdemann, F. M. Ipavich, D. Hovestadt, D. C. Hamilton, and G. Kremser, *Geophys. Res. Lett.* **12**, 325 (1985).
 - [2] B. A. Whalen, W. Bernstein, and P. W. Daly, *Geophys. Res. Lett.* **5**, 55 (1978).
 - [3] G. P. Garbe, R. L. Arnoldy, T. E. Moore, P. M. Kintner, and J. L. Vargo (to be published).
 - [4] G. B. Crew, T. Chang, J. M. Retterer, W. K. Peterson, D. A. Gurnett, and R. L. Huff, *J. Geophys. Res.* **95**, 3959 (1990).
 - [5] T. Chang and B. Coppi, *Geophys. Res. Lett.* **8**, 1253 (1981).
 - [6] P. M. Kintner and D. J. Gorney, *J. Geophys. Res.* **89**, 937 (1984).
 - [7] W. K. Peterson, E. G. Shelley, S. A. Boardsen, D. A. Gurnett, B. G. Ledley, M. Sugiura, T. E. Moore, and J. H. Waite, *J. Geophys. Res.* **93**, 11405 (1988).
 - [8] J. LaBelle, P. M. Kintner, A. W. Yau, and B. A. Whalen, *J. Geophys. Res.* **91**, 7113 (1986).
 - [9] R. L. Arnoldy, K. A. Lynch, P. M. Kintner, J. Vago, S. Chesney, T. E. Moore, and C. J. Pollock, *Geophys. Res. Lett.* **19**, 413 (1992).
 - [10] J. E. Maggs and W. Lotko, *J. Geophys. Res.* **86**, 3439 (1981).
 - [11] S. L. Musher and B. I. Sturman, *Pis'ma Zh. Eksp. Teor. Fiz.* **22**, 537 (1975) [*JETP Lett.* **22**, 265 (1975)].
 - [12] G. J. Morales and Y. C. Lee, *Phys. Rev. Lett.* **35**, 930 (1975).
 - [13] J. M. Retterer, T. Chang, and J. R. Jasperse, *J. Geophys. Res.* **91**, 1609 (1986).
 - [14] D. M. Klumpar, *J. Geophys. Res.* **84**, 4229 (1979).

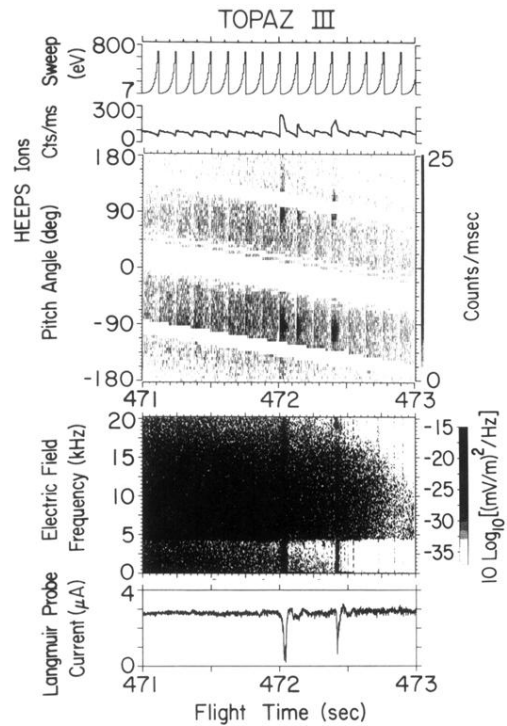


FIG. 1. 2 s of sounding-rocket data at 1012-km altitude. The upper panel (sweep and labeled counts/ms) shows the count rate of a pinch-angle-imaging ion analyzer and the ion energy. The panel labeled “pitch angle” shows as a gray scale, the ion count rate as a function of pitch angle with respect to the geomagnetic field. The panel labeled “electric field” shows the electric-field power spectrum as a gray scale. The bottom panel shows the current drawn by a fixed-bias (+5 V) Langmuir probe.